

# The Inverse Faraday effect in the massive Dirac electrons

Guanxiong Qu<sup>1</sup> and Gen Tatara<sup>1</sup>

<sup>1</sup>*RIKEN Center for Emergent Matter Science (CEMS), Wako 351-0198, Japan.*

(Dated: January 26, 2022)

We study the inverse Faraday effect (IFE) in Dirac Hamiltonian with random impurities using the Keldysh formalism and diagrammatic perturbation theory. The mass term in Dirac Hamiltonian is essential for the IFE, where the spin magnetic moment induced by circularly polarized light is proportional to frequency of the incident light within THz regime. For massive Dirac electrons, the corrections due to the short-range impurities on spin magnetic moment vertex exhibits mixing of spin magnetic moment vertex and spin angular momentum vertex. The spin magnetic density response is divergently enhanced by the vertex corrections near the band edge.

*Introduction.* The Dirac equation[1] successfully describes the dynamics of relativistic electrons. Despite its background in high energy physics, the Dirac Hamiltonian and its variations are widely exploited as low-energy effective Hamiltonians in condensed matter physics, predominantly attributed to its inherent spin(pseudo-spin) orbit interaction. Among variations, Dirac and Weyl semimetals[2–4] which exhibit gapless excitations have drawn much attentions recently[5–8]. The massive Dirac Hamiltonian also describes various gapped systems with quasi-linear band dispersion, *e.g.*, the *L*-point of the Bismuth[9–13].

The inherent spin orbit coupling (SOC) enables the Dirac electrons to exhibit various spin-related responses to the external electric field. For example, the ferromagnetic Dirac Hamiltonian[11, 14] has been employed to study the theory of anomalous Hall effect. The massive Dirac Hamiltonian has been demonstrated a strong spin Hall effect inside the mass gap[10, 13]. In addition to the dc electric field, the optical response of Dirac electrons has also been studied theoretically, especially focusing on the chirality dependent phenomena, *e.g.*, the inverse Faraday effect[15–19] (IFE) and circular photogalvanic effect[17, 20] (CPGE). Nevertheless, the theoretical investigation has been restricted to the massless case of Dirac systems.

The inverse Faraday effect [21, 22] phenomenologically describes the static magnetization induced by the circularly polarized light. The symmetry argument[23] gives a qualitative expression of the induced effective magnetic field:  $\mathbf{M}_{\text{eff}} \sim i\mathcal{E} \times \mathcal{E}^*$  where  $\mathcal{E}$  is the complex electric field. In experiments, the IFE is able to reverse the magnetization of magnets with strong laser pulse[24, 25], providing an optical method of ultrafast magnetization manipulation. As was demonstrated recently, sensitive detection of the effective magnetic field induced by a continuous laser can be carried out electrically through the inverse spin Hall effect[26]. It is, thus, of interest to investigate the IFE in massive Dirac electrons which has been demonstrated to exhibit a large spin Hall effect[10].

The Dirac Hamiltonian is featured by its particle-hole symmetry. The negative energy states correspond to electron vacancies (holes), and thus physical operators are antisymmetric with respect to energy. It turns out, how-

ever, that physical operators are mixed by interactions with its unphysical counterparts which is symmetric with energy. We shall demonstrate that even an energy conserving impurity scattering leads to an entanglement of physical magnetic moment and unphysical spin (angular) vertices[27], resulting in a significant enhancement of magnetic moment response at the band edge. The entanglement is a result of an interference between positive and negative energy states like the *Zitterbewegung*[28] and is unique feature of Dirac electrons. Further, the IFE is known to be dissipative and extrinsic[16, 17, 29], wherefore the IFE of the massive Dirac electrons is also a nice paradigm to study the vertex corrections of Dirac Hamiltonian.

In this letter, we study the spin responses under circularly polarized light in massive Dirac electrons by using the Keldysh Green's function formalism. The spin magnetic density correlates with chirality of the incident light by calculating the second order perturbation of the gauge coupling. The response function holds for general frequency of incident light, while low frequency expansion is employed for an analytical results. The electrons' lifetime and the ladder-type VCs are introduced by the short-range impurities. For impurity correction on the spin magnetic vertex, mixing of the spin vertices in the massive scenario is investigated in detail through concerning the long-range diffusion.

*Model.* We start from the effective Hamiltonian describing the Dirac electrons:

$$\mathcal{H}_0 = \hbar v k_i \rho_1 \otimes \sigma^i + m \rho_3 \otimes \sigma^0, \quad (1)$$

where  $v$  is Fermi velocity and  $m$  is mass term corresponding to half of the band gap[12]. The  $\rho_\mu, \sigma^\nu$  are Pauli matrices spanning the particle-hole and spin space respectively ( $\mu, \nu = 0, 1, 2, 3$ ). Note that the  $\rho_0, \sigma^0$  are identity matrix. The repeated indices indicate summation. The band energy is  $\eta \varepsilon_{\mathbf{k}} \equiv \eta \sqrt{\hbar^2 v^2 k^2 + m^2}$  with  $\eta$  representing the positive (+1) and negative (-1) energy bands.

The impurity scattering is assumed to be random and short-ranged. The impurity potential is

$$V_{\text{imp}} = n_i u \rho_0 \otimes \sigma^0, \quad (2)$$

where  $n_i$  is impurity density and  $u$  is strength of  $\delta$ -function impurities. With the Born approximation, the

retarded self energy[11, 13] is

$$\Im\Sigma^R(\varepsilon) \equiv -\gamma_0(\varepsilon)\rho_0 \otimes \sigma^0 - \gamma_3(\varepsilon)\rho_3 \otimes \sigma^0, \quad (3)$$

where the  $\gamma_0$  and  $\gamma_3$  are

$$\gamma_0(\varepsilon) = \frac{\pi}{2}n_i u^2 \nu(\varepsilon + \mu), \quad (4a)$$

$$\gamma_3(\varepsilon) = \frac{\pi}{2}n_i u^2 \frac{m}{\varepsilon + \mu} \nu(\varepsilon + \mu), \quad (4b)$$

with the density of states is  $\nu(\varepsilon + \mu) \equiv 1/V \sum_{\eta, \mathbf{k}} \delta(\varepsilon + \mu - \eta\varepsilon_{\mathbf{k}})$ .  $V$  is volume of the system. Note that  $\Re, \Im$  denote the real and imaginary components. The density of states of the Dirac Hamiltonian is asymptotically proportional to square of energy,  $\nu(\varepsilon) \propto |\varepsilon| \sqrt{\varepsilon^2 - m^2}$ .  $\gamma_0$  is damping coefficient symmetric with respect to the positive and negative energy bands, while  $\gamma_3$  is anti-symmetric damping coefficient associated with the mass term. Including the self-energy, the retarded Green's function is  $\mathcal{G}_{\mathbf{k}}^R(\omega) = (\hbar\omega + \mu - \mathcal{H}_0 - V_{imp} - i\Im\Sigma^R(\hbar\omega))^{-1}$ .

Although the self-energy is generally energy-dependent, in the following discussion we focus on the scattering effect predominantly at the Fermi surface. Thus, we assume the on-shell condition[30]:  $\mu = \eta\varepsilon_{\mathbf{k}}$ ,  $\varepsilon = 0$ , where the damping coefficients are approximated as constants in energy and have the following relationship:  $\Gamma = \gamma_0 + m/\mu\gamma_3$ . Correspondingly, the electrons' lifetime in on-shell condition is defined as

$$\tau = \frac{\hbar}{2\Gamma} = \frac{\hbar}{\pi n_i u^2 \nu(\mu)} \frac{\mu^2}{\mu^2 + m^2}. \quad (5)$$

The incident light is described by the gauge coupling:

$$H_{em}(\mathbf{x}, t) = -evA_i(\mathbf{x}, t)\rho_1 \otimes \sigma^i, \quad (6)$$

where  $\mathbf{A}(\mathbf{x}, t) = \Re\mathcal{A}e^{i(\mathbf{q}\cdot\mathbf{x} - \Omega t)}$  is the vector potential of incident light. The gauge field is defined by the physical external electric field:  $\mathcal{A} = -i\mathcal{E}/\Omega$ .  $e$  is the elementary charge.

The induced spin magnetic density is calculated through Keldysh formalism. Thus, the expectation value of spin magnetic density is expressed by the equal space-time lesser Green's function:

$$\langle m^k \rangle = -i\hbar \text{Tr} [m^k G^<(\mathbf{x}, t; \mathbf{x}, t)]. \quad (7)$$

where the spin magnetic operator is  $m^k \equiv \rho_3 \otimes \sigma^k$  and its prefactor  $-g^* \mu_B/2$ [12] is neglected for simplicity.  $g^*$  is effective g-factor and  $\mu_B$  is Bohr magneton. Note that the  $G^<$  is the Green's function containing the gauge field which is treated in perturbative expansion. Since the IFE is qualitatively proportional to the cross product of the external electric field[23], it can be traced from the second order perturbation of the gauge coupling in Eq. (7), whose corresponding diagram is shown in Fig. 1.

The spin magnetic density induced by the second order perturbation of the gauge field reads

$$\langle m^k \rangle^{(2)} = -i [\chi_{ij}^k(+\Omega) + \chi_{ji}^k(-\Omega)] \mathcal{E}_i \mathcal{E}_j^*, \quad (8)$$

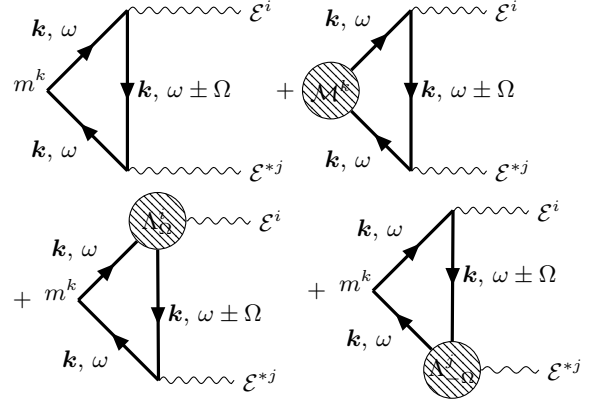


FIG. 1. Diagrammatic representation of the spin magnetic density induced by the circularly polarized light. The first diagram is spin magnetic response without VCs for impurity and the rest are corrections on the spin magnetic vertex and velocity vertices. The shaded circle represents the corrected vertices, see Ref. [31].

where the spin magnetic response function is defined as

$$\chi_{ij}^k(\Omega) \equiv \frac{e^2}{4\hbar\Omega^2 V} \sum_{\mathbf{k}, \omega} \text{Tr} [m^k \mathcal{G}_{\mathbf{k}}(\omega) v_i \mathcal{G}_{\mathbf{k}}(\omega + \Omega) v_j \mathcal{G}_{\mathbf{k}}(\omega)]^<. \quad (9)$$

Note that the velocity operator is  $v_i \equiv \hbar v \rho_1 \otimes \sigma^i$ . The lesser Green's function is given by  $\mathcal{G}_{\mathbf{k}}^<(\omega) = f(\omega) (\mathcal{G}_{\mathbf{k}}^A(\omega) - \mathcal{G}_{\mathbf{k}}^R(\omega))$  with  $f(\omega)$  is the Fermi distribution function.

Utilizing the spherical symmetry of Dirac Hamiltonian and evaluating the trace term in Eq. (9), it is evidenced that the response function is totally anti-symmetric  $\chi_{ij}^k(\Omega) \propto \epsilon_{ijk}$ , corresponding to the anti-symmetry with respect to the chirality of the incident light. The coefficient in Eq. (8) can be rewritten as

$$\chi_{ij}^k(-\Omega) + \chi_{ji}^k(+\Omega) = \chi_{ji}^k(+\Omega) - \chi_{ji}^k(-\Omega). \quad (10)$$

Apparently, only terms which are odd with external frequency  $\Omega$  contributes to the IFE. Expanding the lesser Green's function, the response function  $\chi_{ji}^k$  contains both Fermi surface and Fermi sea contributions[31]. The Fermi sea contribution contains only retarded or advanced Green's functions which is of higher order than the Fermi surface term under the condition  $\Gamma/\mu \ll 1$ . The dominance of Fermi surface contributions also justifies our assumption of the on-shell condition, where the self energy is confined within a small region near the Fermi surface. To obtain an analytical expression, the response function  $\chi_{ji}^k$  is expanded in the limit  $\Omega\tau \ll 1$ . Thus, the leading physical contribution turns out to be linear in  $\Omega$ .

In the zero temperature limit, the spin magnetic den-

sity response function without VCs (Fig. 1) is

$$\chi_{ij}^k(\Omega) = \epsilon_{ijk} \hbar v^2 e^2 \frac{m(\mu^2 - m^2)(2\mu^2 + 3m^2)}{12\mu^3(\mu^2 + m^2)^2} \nu(\mu) \Omega \tau^2. \quad (11)$$

The result (Eq. (11)) indicates that IFE vanishes for massless ( $m = 0$ ) case. Similarly, for massless Weyl semimetal, the photovoltaic chiral magnetic effect can only be induced with unbalanced chemical potential[17]. The induced spin magnetic density changes sign for electron and hole states. Despite the divergence of the lifetime  $\tau$  at the band edge ( $\mu = \pm m$ ), the response function  $\chi_{ij}^k$  is proportional to  $(\mu^2 - m^2)^{1/2}$  and, thus, vanishes at the band edge.

The VCs on spin magnetic vertex and velocity vertex, represented by infinite sums of the ladder diagrams, need to be taken into account for a consistency with inclusion of the self-energy[31]. The corrected spin magnetic vertex and velocity vertex are

$$\mathcal{M}^k = \frac{(\mu^2 + m^2)}{2(\mu^2 - m^2)^2} (9m\mu s^k + (6\mu^2 + 3m^2)m^k), \quad (12a)$$

$$\Lambda_{\Omega}^i = \frac{\mu^2 - m^2}{2(\mu^2 + 2m^2)} \left( 1 - i \frac{\hbar\Omega}{\Gamma} \frac{3(\mu^2 + m^2)}{2(\mu^2 + 2m^2)} \right) v_i, \quad (12b)$$

where the  $s^k \equiv \rho_0 \otimes \sigma^k$  is defined as spin angular operator. In the presence of mass gap, the physical spin magnetic vertex  $m^k$  is coupled with the spin angular vertex  $s^k$  which does not correspond to any physical observables. Although the corrected velocity vertex  $\Lambda_{\Omega}^i$  is also mixed with the spin velocity vertex  $\propto \rho_2 \otimes \sigma^i$ , the mixing coefficient is of the order of  $\Gamma/\mu$  and thus its contribution is neglected[32]. In contrast, the coefficients of  $s^k$  and  $m^k$  vertices are in the same energy scale. Thus, the two spin vertices always entangle with each other except for the massless case where the pairs of spin vertices are decoupled. Vanishing of the mixing can be easily justified by the fact that in massless Dirac electrons the total Hamiltonian is block diagonal. For massive Dirac electrons, the corrected spin magnetic vertex diverges at the band edge

(Eq. (12a)). The divergence can be justified by that at the band edge all the scattering processes are degraded due to the vanish of the states as will be discussed in later section.

Due to the entanglement of spin magnetic and spin angular vertices in the VC (Eq. (12a)), we need to evaluate spin angular response with respect to circularly polarized light by simply replacing the spin magnetic operator with the spin angular operator in Eq. (9). The spin angular response function[31] reads

$$\Pi_{ij}^k(\Omega) = \epsilon_{ijk} \hbar v^2 e^2 \frac{(m^2 - \mu^2)(\mu^2 + 2m^2)}{12\mu^2(\mu^2 + m^2)^2} \nu(\mu) \Omega \tau^2. \quad (13)$$

where we trace the second order perturbation with the gauge field coupling and take out the physical contribution linear with  $\Omega$ . The spin spin angular response function, instead, is an even function with the chemical potential corresponding to the same responses in the positive and negative energy bands and does not vanish in massless limit.

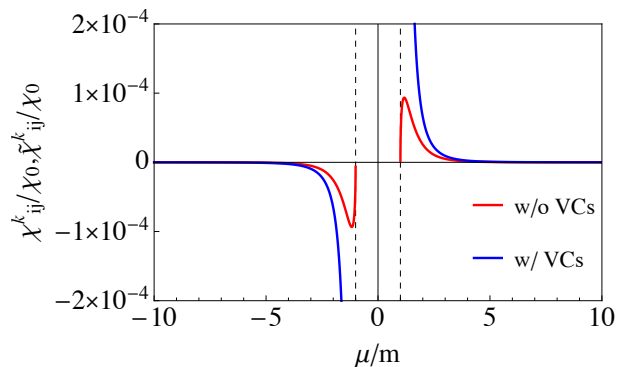


FIG. 2. The spin magnetic response with (Eq. (11)) or without (Eq. (14)) vertex correction and the light frequency is set as  $\Omega\tau_0 = 0.1$ . The unit of the response coefficient is normalized by  $\chi_0 = \hbar e^2 v^2 \tau_0^2 \nu_0$  with  $\nu_0 = m^2/(\pi^2 \hbar^3 v^3)$  and  $\tau_0 = \hbar/(\pi n_i u^2 \nu_0)$ .

The spin magnetic response function with VCs is, thus, calculated below

$$\tilde{\chi}_{ij}^k(\Omega) = \frac{9m\mu(\mu^2 + m^2)}{2(\mu^2 - m^2)^2} \Pi_{ij}^k(\Omega) + \left( \frac{3(2\mu^2 + m^2)(\mu^2 + m^2)}{2(\mu^2 - m^2)^2} + \frac{\mu^2 - m^2}{\mu^2 + 2m^2} \right) \chi_{ij}^k(\Omega). \quad (14)$$

Including the VCs, spin magnetic density still vanishes in massless case and is drastically enhanced in the vicinity of the band gap and shows divergent behavior at the band edge (Fig. 2), attributed to the divergent behavior of the VC on the spin magnetic vertex. Note that the present analysis breaks down only at the band edge due to a divergence of electrons' lifetime.

*Discussion and conclusion.* In presence of mass gap, the VCs of Dirac Hamiltonian involves an entanglement between the original vertex, denoted by  $O$ , and its counterpart vertex obtained from the anti-commutator with the mass term operator,  $\{O, \rho_3 \otimes \sigma^0\}$ . In the case of velocity vertex, the mixing is negligible in order of  $\Gamma/\mu$  and the summation of iterative ladders converge trivially,

while it is the same order as the original vertex for the case of spin and charge (see Ref. [31]) density vertex, resulting in the enhancement at band edge. The entanglement of the vertices in VCs is the consequence of the the mixing between the positive and negative energy states in massive Dirac electrons. The mixing is significant where chemical potential is close to the Dirac point. For example, the corrected spin magnetic vertex (Eq. (14)) has contribution from the spin angular vertex with the order of  $m/\mu$ . and the VCs returns to nearly a constants  $\tilde{\chi}_{ij}^k \sim 4\chi_{ij}^k$ , when  $\mu$  is far from the band edge.

The divergence of VC indicates a long-range diffusion[33]. In fact, considering finite external wavevector  $\mathbf{q}$  and frequency  $\nu$ , the VC of spin magnetic vertex (Eq. (12a)) becomes[31]

$$\mathcal{M}^k(\mathbf{q}, \nu) \simeq \frac{1}{\tilde{D}q^2\tau - i\nu\tilde{\tau} + K} \times \left( \frac{m\mu}{(m^2 + \mu^2)} s^k + \frac{m^2 + 2\mu^2}{3(m^2 + \mu^2)} m^k \right) \quad (15)$$

with normalized diffusion coefficients  $\tilde{D}$  and normalized lifetime  $\tilde{\tau}$  are presented in Ref. [31]. The constant  $K \equiv \frac{2(\mu^2 - m^2)^2}{9(\mu^2 + m^2)^2}$  is the *mass* term of the diffusion kernel, which gives the spin diffusion length  $\lambda_s$ :

$$\lambda_s = \sqrt{\tilde{D}\tau/K} \quad (16)$$

The spin diffusion length diverges as  $\lambda_s \propto (\mu^2 - m^2)^{-1}$  at the band edge for both massive and massless cases. Note that for the massless Dirac Hamiltonian, the band edge return to a single Dirac point ( $\mu = 0$ ). For the massless case, the *mass* term  $K$  is a constant, wherefore the spin density profile drastically decays at the Dirac point without divergence. For the massive Dirac electron, the *mass* term, however, vanishes at the band edge, causing the divergence of the spin density profile.

For massive Dirac electrons, the occurrence of the IFE do not require breaking the inversion symmetry, in contrast to the massless Weyl semimetal[17]. One typical material which could be effectively described by the

Dirac Hamiltonian is the  $L$ -point of bismuth and its alloys[12]. We estimate the induced spin magnetic field  $-g^*\mu_B/2\langle m^z \rangle$  by the circularly polarized light with the experimental parameters in Ref. [34]:  $v = 3.5 \times 10^5$  m/s,  $m = 7.7$  meV,  $g^* \sim 181$ ,  $\tau = 4.2 \times 10^{-14}$  s. The chemical potential is chosen as  $\mu = 160$  meV corresponding to the minimum carrier density available in experiments  $n_0 \sim 10^{19}$  cm $^{-3}$ . For monochromatic light source, we set the frequency to Terahertz regime:  $\Omega = 10$  THz with electric field strength  $|\mathcal{E}| = 3.1$  kV/m ( $I = 1.3 \times 10^4$  W/m $^2$ )[26]. The induced effective magnetic field is  $2.3 \times 10^{-11}$  T. Note that the effective magnetic field can not be detected directly but can be traced by measuring the charge current through the inverse spin Hall effect. For a pulse laser whose electric field strength can rise to  $|\mathcal{E}| = 0.27$  kV/m ( $I = 10^{14}$  W/m $^2$ )[35], the induced effective magnetic field can reach 0.17 T, possibly attributed to the large  $g^*$  of  $L$ -point in bismuth. Our analytical calculation can not be applied to the frequency range of the visible light, due to assumption in the expansion of photon energy  $\Omega\tau \ll 1$ . The extension to the visible light range could rely on the numerical calculations based on the DFT theory[18, 19].

In conclusion, we theoretically study the spin magnetic density induced by the circularly polarized light in massive Dirac electrons with random short-ranged impurities. The induced spin magnetic density only appears in presence of the mass gap and is linear with the photon energy up to TeraHertz (THz) regime. The vertex correction due to short-ranged impurities on the spin magnetic vertex involves the mixing between spin magnetic vertex and spin angular vertex in the massive case. The vertex correction drastically enhances the spin magnetic response in the vicinity of the band edge. Resolving behavior at band edge of massive Dirac Hamiltonian is yet an issues to be solved in future.

## ACKNOWLEDGMENTS

The authors would like to thank Prof. M. Hayashi and Dr. J Fujimoto for their kind correspondences. This work was supported by Grants-in-Aid for Scientific Research (B) (No. 21H01034) from the Japan Society for the Promotion of Science.

- 
- [1] P. A. M. Dirac, Proceedings of the Royal Society of London. Series A, Containing Papers of a Mathematical and Physical Character **117**, 610 (1928).
  - [2] A. Burkov and L. Balents, Physical review letters **107**, 127205 (2011).
  - [3] B.-J. Yang and N. Nagaosa, Nature communications **5**, 1 (2014).
  - [4] N. Armitage, E. Mele, and A. Vishwanath, Reviews of Modern Physics **90**, 015001 (2018).
  - [5] M. Brahlek, N. Bansal, N. Koirala, S.-Y. Xu, M. Neupane, C. Liu, M. Z. Hasan, and S. Oh, Physical review letters **109**, 186403 (2012).
  - [6] L. Wu, M. Brahlek, R. V. Aguilar, A. Stier, C. Morris, Y. Lubashevsky, L. Bilbro, N. Bansal, S. Oh, and N. Armitage, Nature Physics **9**, 410 (2013).
  - [7] Z. Liu, B. Zhou, Y. Zhang, Z. Wang, H. Weng, D. Prabhakaran, S.-K. Mo, Z. Shen, Z. Fang, X. Dai, *et al.*, Science **343**, 864 (2014).
  - [8] Z. Liu, J. Jiang, B. Zhou, Z. Wang, Y. Zhang, H. Weng, D. Prabhakaran, S. K. Mo, H. Peng, P. Dudin, *et al.*, Nature materials **13**, 677 (2014).
  - [9] Y. Fuseya, M. Ogata, and H. Fukuyama, Physical review

- letters **102**, 066601 (2009).
- [10] Y. Fuseya, M. Ogata, and H. Fukuyama, *J. Phys. Soc. Jpn.* **81**, 093704 (2012).
- [11] J. Fujimoto and H. Kohno, *Phys. Rev. B* **90**, 214418 (2014).
- [12] Y. Fuseya, M. Ogata, and H. Fukuyama, *Journal of the Physical Society of Japan* **84**, 012001 (2015).
- [13] T. Fukazawa, H. Kohno, and J. Fujimoto, *J. Phys. Soc. Jpn.* **86**, 094704 (2017).
- [14] A. Crépieux and P. Bruno, *Physical Review B* **64**, 014416 (2001).
- [15] W.-K. Tse and A. H. MacDonald, *Physical review letters* **105**, 057401 (2010).
- [16] T. Misawa, T. Yokoyama, and S. Murakami, *Physical Review B* **84**, 165407 (2011).
- [17] K. Taguchi, T. Imaeda, M. Sato, and Y. Tanaka, *Physical Review B* **93**, 201202 (2016).
- [18] F. Freimuth, S. Blügel, and Y. Mokrousov, *Phys. Rev. B* **94**, 144432 (2016).
- [19] M. Berritta, R. Mondal, K. Carva, and P. M. Oppeneer, *Phys. Rev. Lett.* **117**, 137203 (2016).
- [20] P. Hosur, *Physical Review B* **83**, 035309 (2011).
- [21] L. Pitaevskii, *Sov. Phys. JETP* **12**, 1008 (1961).
- [22] P. Pershan, *Physical Review* **130**, 919 (1963).
- [23] L. D. Landau, J. Bell, M. Kearsley, L. Pitaevskii, E. Lifshitz, and J. Sykes, *Electrodynamics of continuous media*, Vol. 8 (elsevier, 2013).
- [24] A. Kimel, A. Kirilyuk, P. Usachev, R. Pisarev, A. Balbashov, and T. Rasing, *Nature* **435**, 655 (2005).
- [25] A. Kirilyuk, A. V. Kimel, and T. Rasing, *Reviews of Modern Physics* **82**, 2731 (2010).
- [26] M. Kawaguchi, H. Hirose, Z. Chi, Y.-C. Lau, F. Freimuth, and M. Hayashi, *arXiv preprint arXiv:2009.01388* (2020).
- [27] M. Ramana and A. Rajagopal, *Journal of Physics C: Solid State Physics* **14**, 4291 (1981).
- [28] J. J. Sakurai, *Advanced quantum mechanics* (Pearson Education India, 2006).
- [29] K. Taguchi and G. Tatara, *Physical Review B* **84**, 174433 (2011).
- [30] J. Fujimoto and M. Ogata, *arXiv preprint arXiv:2106.04050* (2021).
- [31] See Supplemental Material at for The Inverse Faraday effect in the massive Dirac electrons.
- [32] J. Fujimoto, *Physical Review B* **97**, 104421 (2018).
- [33] P. Coleman, *Introduction to many-body physics* (Cambridge University Press, 2015).
- [34] C. et al., (unpublished).
- [35] S. Mangin, M. Gottwald, C. Lambert, D. Steil, V. Uhlř, L. Pang, M. Hehn, S. Alebrand, M. Cinchetti, G. Malinowski, *et al.*, *Nature materials* **13**, 286 (2014).